IOP PUBLISHING JOURNAL OF PHYSICS: CONDENSED MATTER

J. Phys.: Condens. Matter **19** (2007) 375107 (13pp) doi:10.1088/0953-8984/19/37/375107

Utilizing ultrathin DNA/poly-lysine multilayer films to create liquid/liquid interfaces: spectroscopic characterization, interfacial reactions and nanoparticle adsorption

Hye Jin Lee, Alastair W Wark and Robert M Corn

Department of Chemistry, University of California-Irvine, Irvine, CA 92697, USA

E-mail: rcorn@uci.edu

Received 15 December 2006, in final form 15 January 2007
Published 13 August 2007
Online at stacks.iop.org/JPhysCM/19/375107

Abstract

Alternating electrostatic multilayer adsorption of poly-L-lysine (pLys) and DNA is used to create well-defined biopolymer multilayers for use as an ultrathin aqueous phase in liquid–liquid interfacial measurements. The molecular structure and thickness of the polyelectrolyte multilayers are determined using a combination of polarization modulation FT-IR reflection-absorption spectroscopy (PM-FTIRRAS) and FT-surface plasmon resonance (FT-SPR) thickness measurements. Electroactive species such as ferri/ferrocyanide ions can be incorporated into the DNA/pLys polyelectrolyte multilayers. The ion transport activity of these electroactive films when in contact with 1,2-dichoroethane is verified by electrochemical measurements. Micron-sized patterns of these multilayers are created by either photopatterning, vapour-deposited spot patterning or microfluidic stencil processing, and are used in conjunction with fluorescence and surface plasmon resonance imaging (SPRI) to monitor (i) the intercalation of dye molecules into DNA/pLys ultrathin films, (ii) the electrostatic adsorption of gold nanoparticles onto DNA/pLys multilayers and (iii) the spatially controlled incorporation and reaction of enzymes into patterned biopolymer multilayers.

(Some figures in this article are in colour only in the electronic version)

1. Introduction

The formation of well-defined polyelectrolyte multilayers by the process of electrostatic layer by layer (LbL) deposition has become a powerful method for the fabrication of ultrathin polymer films [1–3]. The overall thickness of these films can be controlled with nanometre precision. LbL deposition can use a wide variety of charged materials including polymers,

biopolymers and metallic and semiconducting nanoparticles to create thin films with unique optical and electronic properties on many types of surfaces [4–8]. Most of the polymers used in the fabrication of LbL films are hydrophobic; however, LbL films formed from biopolymers such as DNA and polypeptides are hydrophilic. For example, we have previously investigated poly-L-lysine/poly-L-glutamic acid (pLys/pGlu) multilayers, and have shown that hydrophilic electroactive species capable of transporting charge can be incorporated into these multilayers [9, 10]. These ultrathin films can be used in immiscible liquid–liquid electrochemical experiments when brought into contact with an organic electrolyte solution [9–13].

We report here the creation of another biopolymer multilayer for use as an ultrathin aqueous phase in liquid–liquid measurements: DNA/pLys multilayers. DNA is a naturally occurring anionic biopolymer and a great choice for the fabrication of LbL multilayers because we can vary its length very easily, and use either single stranded DNA (ssDNA) or double stranded DNA (dsDNA) which have different polymer backbone persistence lengths. The use of DNA in multilayers opens up new possibilities for applications in biosensing. Several researchers have reported the combined use of DNA with pLys [14–18] and other positively charged polyelectrolytes [19–23] to prepare ultrathin LbL films for applications including cell culture studies, therapeutics and gene delivery and DNA nanodevices.

In this paper, we demonstrate that DNA/pLys multilayers of well-controlled thickness can be created on gold surfaces. Various species including electroactive molecules, enzymes, fluorescent dyes and gold nanoparticles can be incorporated into these ultrathin films. The DNA/pLys multilayers are first characterized using a combination of polarization modulation FT-IR reflection-absorption spectroscopy (PM-FTIRRAS) and FT-SPR thickness measurements. The liquid–liquid electrochemical activity of these thin films when in contact with 1,2-dichoroethane (1,2-DCE) is verified by the electrochemical cycling of ferri/ferrocyanide ions incorporated into the multilayer film. We also demonstrate that these multilayers can be patterned on a micrometre scale with either photopatterning or PDMS microfluidics. These patterned surfaces can be used in the formation of biosensor microarrays in conjunction with fluorescent intercalating dyes. As two additional examples of the utility of these multilayers, we demonstrate (i) surface plasmon resonance imaging (SPRI) measurements of the patterned electrostatic adsorption of gold nanorods onto DNA/pLys multilayers created on modified gold surfaces and (ii) fluorescence measurements of spatially controlled reaction and incorporation of enzymes into the polyelectrolyte multilayers.

2. Experimental considerations

Materials

11-Mercaptoundecanoic acid (MUA; Sigma-Aldrich), 11-amino-1-undecanethiol hydrochloride (MUAM; Dojindo), potassium ferricyanide ($K_3Fe(CN)_6$), potassium ferrocyanide ($K_4Fe(CN)_6$, Fluka), tetrabutylammonium tetraphenylborate (TBATPB; Fluka) and tetrabutylammonium chloride (TBACl; Sigma-Aldrich), 1,2-dichloroethane (1,2-DCE, Sigma-Aldrich), poly-L-lysine hydrobromide (pLys, MW 34 300, Sigma-Aldrich), 9-fluorenylmethoxycarbonyl-*N*-hydroxysuccinimide (Fmoc-NHS; Novabiochem), polydimethylsiloxane (PDMS) curing agent and prepolymer (Sylgard 184, Dow Corning, Midland, MI) were all used as-received. Immunopure avidin horseradish peroxidase (HRP) conjugated (Pierce), EZ link NHS-Biotin (Pierce), Quantablu fluorogenic peroxidase substrate (Pierce), YOYO-1 iodide (Invitrogen), sonicated calf thymus dsDNA (GE Healthcare), dsDNA from salmon testes (Sigma-Aldrich), 36mer unmodified ssDNA sequences (HPLC purified, Integrated DNA Technologies) and cer-

tified molecular biology agarose (Bio-Rad) were all used as-received and diluted to a desired concentration prior to use. All rinsing steps were performed with either Millipore filtered water or absolute ethanol. All experiments were performed at room temperature unless stated otherwise.

Preparation of gold thin film

Thin gold films for FT-SPR (41 nm) and SPR Imaging (45 nm) measurements were prepared by vapour deposition of gold onto SF-10 glass slides (18 mm × 18 mm) using a Denton DV-502A metal evaporator with a 1 nm underlayer of chromium. For PM-FTIRRAS, fluorescence imaging and electrochemical measurements, commercial gold slides (5 nm of Cr, 100 nm of Au from evaporated metal films) were employed. Prior to use, each commercial gold slide was cleaned in piranha solution (3:1 mixture of concentrated H_2SO_4 and 30% H_2O_2) followed by rinsing with water. Gold surfaces were then modified with a self-assembled alkanethiol monolayer (MUA or MUAM) by immersing the slide in a 1 mM ethanolic solution overnight.

Creation of DNA/pLys ultrathin films

DNA/pLys multilayer films were formed by the electrostatic adsorption of alternating layers of pLys and DNA; gold surfaces modified with a well-packed monolayer of MUA or MUAM were exposed to alternating solutions of pLys and DNA for 30 min. After each exposure, the surface was thoroughly rinsed using water and dried under a N_2 stream. Sonicated calf thymus dsDNA (75 μg ml^{-1}), dsDNA from salmon testes (75 μg ml^{-1}), 36mer ssDNA (2 μM) and pLys (2 mg ml^{-1}) buffered in a 0.1 M phosphate solution (pH 8) were used.

Preparation of patterned DNA/pLys ultrathin films

Three different methods were developed to fabricate patterned DNA/pLys multilayers on MUAM-modified gold surfaces. In a first approach, a modified version of a multistep chemical protection/deprotection process described previously [24] was used to create patterned biopolymer multilayers. 3 mM Fmoc-NHS in triethanolamine (TEA; pH 7) was first reacted with the MUAM surface to form a hydrophobic background. The Fmoc layer was then exposed to UV light through a quartz mask containing 100 μm × 100 μm and 25 μm × 25 μm features for 1 h to create bare gold patches surrounded by the Fmoc background. Next, the bare gold patches were reacted with MUAM for 2 h followed by multilayer assembly using dsDNA from salmon testes. The final layer was dsDNA, after which the multilayer was reacted with YOYO-1 fluorescent dye (1 mM buffered in 0.1 M phosphate buffer, pH 8) for 30 min. The specific intercalation of YOYO-1 dye into dsDNA layers was then measured using fluorescence microscopy with a fluorescein isothiocyanate (FITC) filter (λ_{Em} = 530 nm). In a second approach, LbL assembly was performed on an array of gold spots prepared on a hydrophobic-coated glass slide. As described previously [25], a 0.09% (w/w) solution of Cytop (Asahi Glass Company) dissolved in CTL-180 solvent (Asahi Glass Company) was spin-coated onto clean SF10 glass slides with an initial spin rate of 500 rpm for 5 s then manually ramping to 5000 rpm and spinning for a further 50 s. The Cytop-coated glass was baked at 190 °C for 1 h. A thin gold film (45 nm) with a 1 nm underlayer of chromium was then vapour-deposited onto the Cytop-coated slide through a mask featuring a pattern of 750 μm diameter circles with a centre-to-centre separation of 1360 μm. The resulting gold patterned slides were placed into an ethanolic MUAM solution for 2 h. 40 nl solutions of dsDNA from calf thymus and pLys were then sequentially delivered onto each MUAM spot using a pneumatic pico-pump. The resulting multilayer spot patterns were utilized in conjunction with *in situ*

SPRI measurements to investigate the specific electrostatic adsorption of gold nanorods. The third approach utilized PDMS microfluidics to create parallel lines of multilayer films on gold surfaces. The microfluidic channels were fabricated as described previously [26]. First, a set of parallel microchannels was attached to the MUAM modified gold surface. Alternate solutions of dsDNA from salmon testes and pLys were delivered into each microchannel using a simple differential pumping system to create lines of dsDNA/pLys multilayers. 75 μg ml^{-1} dsDNA from salmon testes and 2 mg ml^{-1} pLys buffered in 0.1 M phosphate buffer (pH 8) were used. The dimensions of the microchannels were 75 μm wide by 35 μm deep with a spacing of 100 μm between channels. The biopolymer multilayers (total seven layers including MUAM) with a final layer of pLys were then reacted with 2 mM NHS-biotin in TEA buffer (pH 7). 100 nM avidin modified HRP in phosphate buffer with 100 mM NaCl (pH 7.4) was then injected into each microchannel to react with the biotinylated multilayer film for 30 min, which created lines of surface attached HRP. This first set of PDMS microchannels was peeled off and the chip surface rinsed with water and dried under a N_2 stream. A second set of microfluidic channels was then placed perpendicular to the HRP line array. Next, 2% (w/w) agarose solution (1 ml) was heated to 60 °C followed by the addition of 500 μl of stock solution of QuantaBlu fluorogenic peroxidase substrate. Aliquots (2 μl) of this mixture were immediately flowed through each microchannel. Following gelification after 30 min of cooling, the second set of PDMS microchannels was peeled off to create a pattern of dsDNA/pLys film/hydrogel interfaces with dimensions of 75 μm × 75 μm where the two phases intersect. These patterned interfaces created on gold surfaces were used for the study of an interfacial HRP enzyme reaction using fluorescence microscopy.

Preparation of gold nanorods

Colloidal solutions of gold nanorods were prepared following the procedures described previously by El-Sayed *et al* [27]. Hexadecyltrimethylammoniumbromide (CTAB), sodium borohydride ($NaBH_4$), L-ascorbic acid, silver nitrate ($AgNO_3$) and hydrogen tetrachloroaurate(III) hydrate ($HAuCl_4$) were all used as-received from Sigma-Aldrich. Gold seed solution was first prepared by mixing 5 ml of 0.0005 M $HAuCl_4$ with 5 ml of 0.2 M CTAB solution. Under vigorous stirring, 0.60 ml of ice-cold 0.01 M $NaBH_4$ was quickly added and stirred for an additional 2 min. The nanorod growth solution was prepared by adding 5 ml of 0.2 M CTAB and 5 ml of 0.001 M $HAuCl_4$ to 0.2 ml of 0.004 M $AgNO_3$. To this solution, 70 μl of 0.0788 M L-ascorbic acid was added, changing the solution from dark yellow to colourless. A 12 μl aliquot of seed solution was then added to the growth solution, which slowly changed colour over a period of around 1 h. Prior to performing SPRI measurements, excess CTAB was removed from the nanorod solutions by twice centrifuging the colloidal solution, extracting the supernatant and resuspending in water prior to performing SPR imaging experiments. The final solution had an absorbance of 1.7 at 809 nm using a 1 cm path length cell. All solutions were prepared using Millipore water and kept at 27–29 °C prior to centrifugation.

PM-FTIRRAS measurements

Grazing angle PM-FTIRRAS measurements were performed using a Mattson RS-1 spectrometer and optical layout described elsewhere [28, 29]. Before acquiring each *ex situ* spectrum, the DNA/pLys modified gold slides were thoroughly rinsed with water and dried under a N_2 stream. Spectra were collected using a HgCdTe detector, averaging 1000 scans acquired at a resolution of 4 cm^{-1}.

Electrochemical measurements

A standard three-electrode cell configuration was employed with a gold slide as the working electrode, a Pt wire counter electrode and an Ag/AgCl reference electrode inserted in a liquid junction built between a 10 mM TBATPB organic supporting electrolyte and a 10 mM TBACl aqueous electrolyte. Cyclic voltammetry was performed using a computer-controlled potentiostat (Autolab, Eco Chemie). All applied potentials were defined with respect to Ag/AgCl. $Fe(CN)_6^{3-/4-}$ was incorporated into the DNA/pLys multilayer by immersion into a 1 mM solution of 1:1 $K_3Fe(CN)_6$ and $K_4Fe(CN)_6$ buffered in 0.1 M phosphate buffer (pH 5.6) for 30 min. The slide was finally rinsed with water, dried under a nitrogen stream and mounted into the cell.

SPR imaging measurements

An SPR imager (GWC Technologies) was used for investigating adsorption of gold nanorods onto dsDNA/pLys ultrathin films created on MUAM modified gold surfaces. As described previously [30], a collimated p-polarized light impinges onto a prism/gold thin film/flow cell assembly at a fixed incident angle near the SPR angle. The reflected light is then passed through a narrow band-pass filter (830 nm) and collected with a CCD camera. All SPR images were acquired using the software package Digital Optics V++ 4.0 and analysed using NIH Image V.1.63 software. A solution of gold nanorods in water was injected and then allowed to adsorb electrostatically onto the dsDNA/pLys multilayers for 20 min before rinsing with water. SPRI difference images were obtained by subtracting images acquired before and after adsorption of the gold nanorods.

FT-SPR measurements

FT-SPR measurements were performed using a Bruker Vector 22 FTIR spectrometer equipped with a halogen light source and NIR polarizing optics [31]. The light reflected from a prism/gold thin film/flow cell assembly was collected using an InGaAs photodiode. FT-SPR reflectivity curves were obtained at a fixed incident angle by first collecting a background scan with the incident light s-polarized; a sample scan was then collected on rotating the light to p-polarized. All FT-SPR spectra are the average of 32 scans acquired at 8 cm^{-1} resolution. Shifts in the FT-SPR reflectivity minimum due to localized changes in refractive index and film thickness at the gold surface were analysed by fitting a small region near the minimum to a quadratic.

3. Results and discussion

3.1. Multilayer formation and characterization

The DNA/pLys multilayer films were formed on gold substrates by sequential electrostatic adsorption. The gold surfaces were first modified with either MUAM or MUA to create a charged surface. The substrates were then alternately exposed to solutions of pLys and DNA (see figure 1). Three types of DNA were used to form the multilayers: 36mer synthetic ssDNA, 3 kb sonicated calf thymus dsDNA and 2 kb dsDNA from salmon testes. Ultrathin films of up to 20 layers (10 pLys + 10 DNA) were created. Film formation was characterized using three different measurements: PM-FTIRRAS, FT-SPR and electrochemistry. Some examples of the characterization results are shown here.

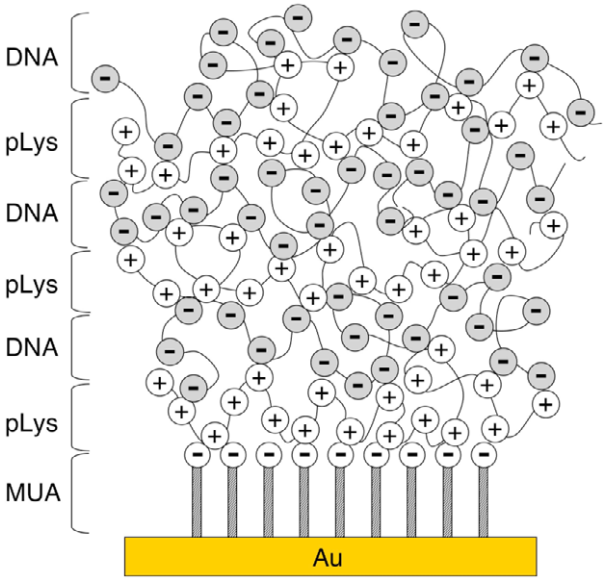

Figure 1. A simplified schematic showing layer by layer formation of DNA/pLys ultrathin films assembled on a gold surface modified with an alkanethiol monolayer such as MUA and MUAM. The DNA/pLys multilayers were created by the sequential adsorption of pLys and DNA.

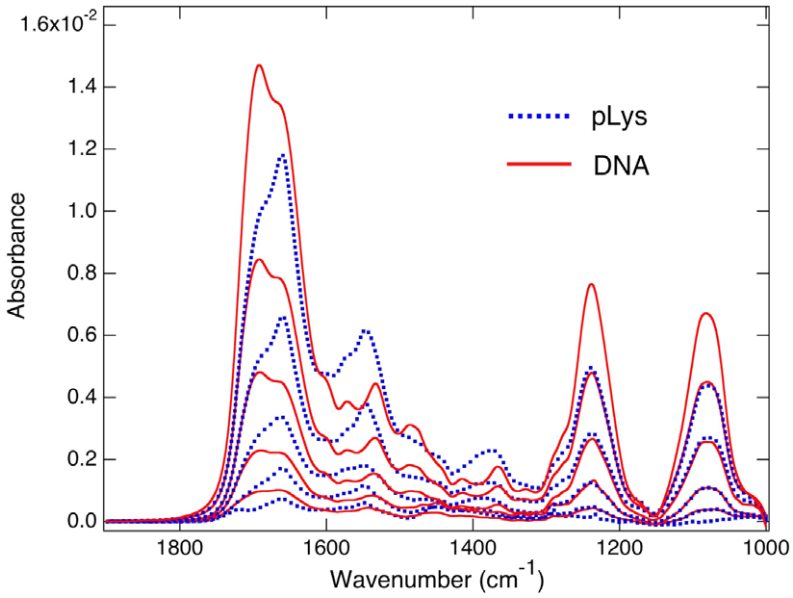

Figure 2. PM-FTIRRAS spectra of ssDNA/pLys multilayers created on a gold surface modified with a well-packed monolayer of MUA. The layer assembly was achieved by exposing the surface to alternating solutions of pLys (2 mg ml^{-1}) and 36mer ssDNA (2 μM) for 30 min.

PM-FTIRRAS measurements. PM-FTIRRAS measurements were taken to determine the film structure during the LbL deposition process. Figure 2 shows a set of PM-FTIRRAS data taken during the formation of a 10-layer DNA/pLys film. In this instance, 36mer ssDNA

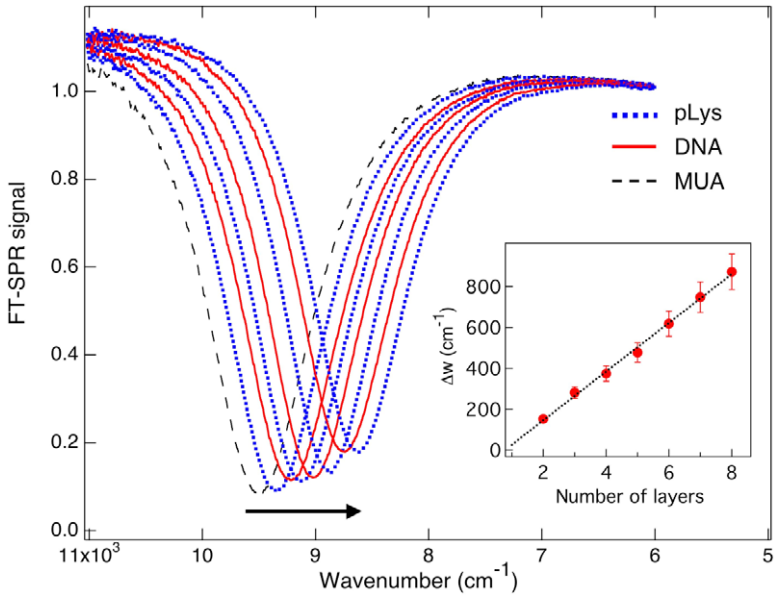

Figure 3. A series of *in situ* FT-SPR spectra measured at a fixed incident angle of 52.68° for the sequential adsorption of alternating layers of positively charged pLys and negatively charged 36mer ssDNA onto a MUA-modified gold film. Each spectrum is the average of 32 scans collected at 8 cm^{-1} resolution. The inset is a plot of the wavenumber shift in the position of the FT-SPR signal minimum measured for each layer with respect to the MUA layer, which is numbered as the first layer on the gold surface. Each subsequent wavenumber shift was correlated to layer thickness using Fresnel calculations [31].

was used. Following the deposition of the first pLys monolayer on the MUA modified gold surface, the PM-FTIRRAS spectra alternated in a regular fashion with each subsequent addition of ssDNA and pLys. The PM-FTIRRAS spectra from pLys-terminated multilayers showed increases in two pronounced peaks at 1660 and 1545 cm^{-1} due to the amide I and II bands of the polypeptide, and the DNA-terminated multilayers showed increases in the two phosphate bands at 1238 and 1046 cm^{-1}, as well as purine ring bands at 1485 and 1365 cm^{-1}. Similar increasing trends were also observed for PM-FTIRRAS measurements where the ssDNA used in the DNA/pLys LbL assembly was replaced with longer dsDNA from both salmon testes and calf thymus. The consistency of the PM-FTIRRAS spectra during the LbL growth process demonstrates that the internal molecular structure of the thin film remains constant with thickness.

FT-SPR thickness measurements. FT-SPR measurements were taken in conjunction with PM-FTIRRAS measurements during the LbL process to determine the film thickness of each pLys and 36mer ssDNA monolayer. We have shown previously that the FT-SPR spectrum is very sensitive to changes in the multilayer film thickness [31]. The wavenumber shift in the minimum position of the FT-SPR spectra can be used to calculate the thickness of each additional monolayer using Fresnel calculations. The *in situ* FT-SPR spectra obtained during the LbL deposition of a ssDNA/pLys film (a total of eight layers including MUA) is shown in figure 3. The measured wavenumber shift was found to be very similar for both the ssDNA and pLys layers with an average shift of 119 ± 20 cm^{-1} after each additional monolayer (see figure 3 inset). A five-phase Fresnel calculation (SF10 prism/gold/MUA/multilayer film/water) was used to determine a thickness of 2.0 ± 0.2 nm for each of the pLys and ssDNA monolayers

with an overall thickness of 14.0 nm for the seven-layer ssDNA/pLys film. A uniform change in thickness of both the pLys and ssDNA layers with increasing layer number was observed for films containing up to 10 layers. Comparison of these results with previous experiments studying the formation of pLys/pGlu multilayer thin films [9, 10] shows the pLys film thickness to be very similar; however, the thickness of the pGlu layers (1.1 nm; ∼70 cm^{-1} shift) is significantly less than the ssDNA layers created in this study.

Electrochemical measurements. The third characterization experiment that we performed on the DNA/pLys multilayers was a set of electrochemical measurements to demonstrate the ion and electron transport capabilities of the films. As in our previous paper on pLys/pGlu multilayers [9, 10], ferri/ferrocyanide redox shuttles were incorporated in the multilayer film. In the present study, multilayers were formed by sequential adsorption of dsDNA from calf thymus and pLys onto a MUAM (positively charged alkanethiol) modified gold surface. The incorporation of ferri/ferrocyanide ions into the bulk of the DNA/pLys multilayer films could be verified with PM-FTIRRAS measurements as previously reported [10]. The resulting electroactive multilayer coated gold slide was dried with N_2 and then brought into contact with 1,2-DCE to form a liquid–liquid interface. The three-electrode electrochemical cell is described in Cell 1 with TBATPB and TBACl used as supporting electrolytes.

$$\mathrm{Ag/AgCl}\,\Big|\,\underbrace{\begin{array}{c}\text{10 mM TBACl}\\ \underbrace{\text{in water}}\end{array}}_{\text{organic reference electrolyte}}\,\Big|\,\underbrace{\begin{array}{c}\text{1,2 DCE}\\ \underbrace{\text{10 mM TBATPB}}\end{array}}_{\text{organic phase}}\,\Big\|\,\underbrace{\begin{array}{c}\text{dsDNA-pLys film}\\ \text{created on MUAM}\\ \underbrace{\mathrm{Fe(CN)_6^{3-/4-}}}\end{array}}_{\text{aqueous phase}}\,\Big|\,\mathrm{Au}$$

(Cell 1)

Figure 4 shows a representative cyclic voltammogram (CV) obtained from a 15-layer film containing ferri/ferrocyanide ions at a scan rate of 100 mV s^{-1}. The observation of a well-defined CV requires a combination of electron transfer across the gold/multilayer film interface and ion transfer across the multilayer film/DCE interface. In the absence of ferri/ferrocyanide ions, only a very small non-Faradaic current was observed. It is difficult to separately investigate the charge transfer processes occurring across each interface; however, the observation of a linear relationship between the cathodic peak current versus scan rate (data not shown) rules out any diffusional behaviour related to interfacial ion transport. The transfer of the highly charged and hydrophilic ferri/ferrocyanide ions into 1,2-DCE is highly unfavourable due to a large Gibbs transfer energy; more likely is the facilitated ion transfer of the organic phase supporting electrolyte ions (TBA^+, TPB^-) to the charged DNA/pLys multilayer film. This facilitated ion transfer would greatly reduce the potential drop across the film/DCE interface.

Further analysis of the CV in figure 4 reveals a peak to peak separation (ΔE_p) of 94 mV. This number typically varied over the range 90–110 mV for different samples, but was independent of the total number of layers in the thin film. A ΔE_p of ∼60 mV is expected for reversible redox behaviour of the ferri/ferrocyanide couple at an unmodified gold electrode surface, but larger peak to peak separations due to slower interfacial electron transfer kinetics have been observed at gold electrodes that have been chemically modified with a well-packed self-assembled monolayer [9, 32]. The additional 35 mV of ΔE_p can therefore be attributed to a combination of residual potential drop across the film/DCE interface and slower electron transfer kinetics at the gold/film interface due to the presence of an alkanethiol monolayer.

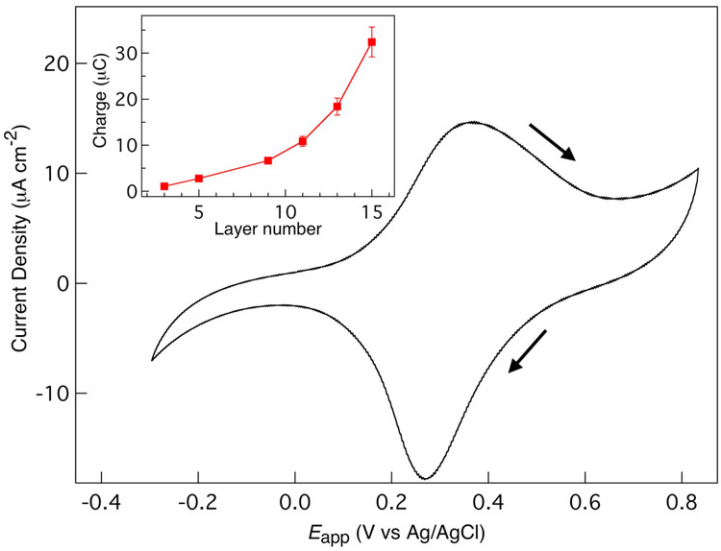

Figure 4. A representative cyclic voltammogram obtained for a dsDNA/pLys ultrathin film (total of 15 layers including MUAM) into which ferri/ferrocyanide ions have been incorporated. The potential sweep rate was 100 mV s^{-1}.The inset shows a plot of charge as a function of layer number. The first layer on the gold surface is a monolayer of MUAM, which was sequentially reacted with dsDNA from calf thymus and pLys with a final top layer of pLys.

For thicker films, the total charge transfer measured for the oxidation and reduction reactions during a CV remained equal, but asymmetric differences in the anodic and cathodic peak shapes became more pronounced as seen in figure 4. This asymmetry is attributed to differences in the amount and distribution of immobilized charge in the dsDNA/pLys multilayer films between the oxidized and reduced states. The inset in figure 4 shows the increase in cathodic charge measured from CV measurements at a fixed scan rate of 100 mV s^{-1} for dsDNA/pLys films ranging from 3 to 15 layers. This monotonic but nonlinear increase indicates that the total concentration of ferri/ferrocyanide ions within the multilayer must be changing with film thickness, and was roughly estimated to be 28 mM for a three-layer film (MUAM, dsDNA, pLys) and 100 mM for a 15-layer film. These values are in good agreement with previous *in situ* PM-FTIRRAS measurements of ferri/ferrocyanide ion concentrations in pLys/pGlu thin films [10].

3.2. Multilayer patterning, adsorption and reaction

The utility of the DNA/pLys films in controlling the chemistry at the liquid–liquid interface is demonstrated with three examples: the intercalation of fluorescent dye molecules into interfacial dsDNA, the patterned adsorption of gold nanorods and an interfacial enzymatic reaction. All three methods utilize patterned surfaces, which can be fabricated by three different methodologies; photopatterning, the use of vapour deposited spot patterns and PDMS microfluidic stencils.

Photopatterning and fluorescent dye intercalation. Patterned dsDNA/pLys multilayer films can be created by photopatterning the underlying alkanethiol monolayer. For example, figure 5(a) outlines a multistep methodology that is described in detail in section 2: MUAM, Fmoc, UV light, backfilling with MUAM and using it to make electrostatic multilayers

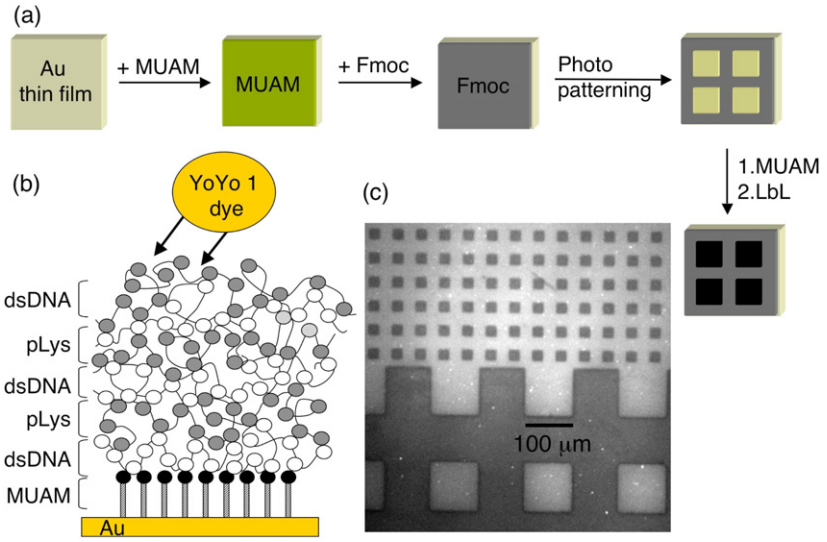

Figure 5. (a) A schematic showing the multistep process used for creating photopatterned dsDNA/pLys ultrathin films on MUAM modified gold surfaces. First, a MUAM modified slide was reacted with Fmoc-NHS followed by exposure to UV light through a quartz mask containing 100 μm $\times$ 100 μm and 25 μm $\times$ 25 μm features to create bare gold patches surrounded by the Fmoc background. The bare gold patches were then exposed sequentially to MUAM, dsDNA, pLys, dsDNA, pLys and dsDNA (a total of six layers including MUAM). The final dsDNA layer was then reacted with YOYO-1 fluorescent dye. (b) Schematic representation of YOYO-1 fluorescent dye intercalated in the dsDNA/pLys film. (c) A fluorescence image showing the intercalation of YOYO-1 dye with dsDNA layers.

composed of a total of six layers (MUAM and alternating dsDNA (salmon testes) and pLys layers). The patterned dsDNA/pLys films surrounded by a Fmoc background were then exposed to an intercalating dsDNA dye, YOYO-1 (see scheme in figure 5(b)). The resulting fluorescent image shown in figure 5(c) demonstrates the intercalation of YOYO-1 dye only at the dsDNA/pLys areas on the surface with negligible nonspecific adsorption of the dye onto the background. Features down to 25 μm could easily be created.

Gold nanorod adsorption. dsDNA/pLys multilayers were used to create a micrometre-scale patterned gold nanorod monolayer by electrostatic interfacial adsorption. The gold nanorods were synthesized via the process of El Sayed *et al* [27] and were characterized with UV–vis absorption spectroscopy ($\lambda_{max} = 806$ and 509 nm) and TEM (average rod length, 44 ± 14 nm; aspect ratio, 3.6 ± 0.8) as shown in figure 6. SPRI measurements were performed to demonstrate that the dsDNA/pLys films can be used to control nanorod adsorption (figure 7). For this experiment, dsDNA/pLys multilayers were created on MUAM modified gold spot arrays. The SPRI difference image shown in the inset of figure 7 was obtained following exposure of the patterned multilayer surface to a solution of gold nanorods. A very large increase in $\Delta\%R$ was observed (30%) only at the top two rows where the films were terminated with a dsDNA monolayer (i.e. MUAM–dsDNA–pLys–dsDNA). Negligible signal change was observed on the remaining spots composed of three layers terminating with pLys; this is due to the fact that the chemical synthesis of the nanorods results in a surrounding layer of positively charged surfactant (CTAB) which is thus electrostatically attracted to the negatively charged surface spots (dsDNA) but not to the positively charged pLys termination films. This approach could potentially be used to prepare ultrathin films with unique optical and electrical properties.

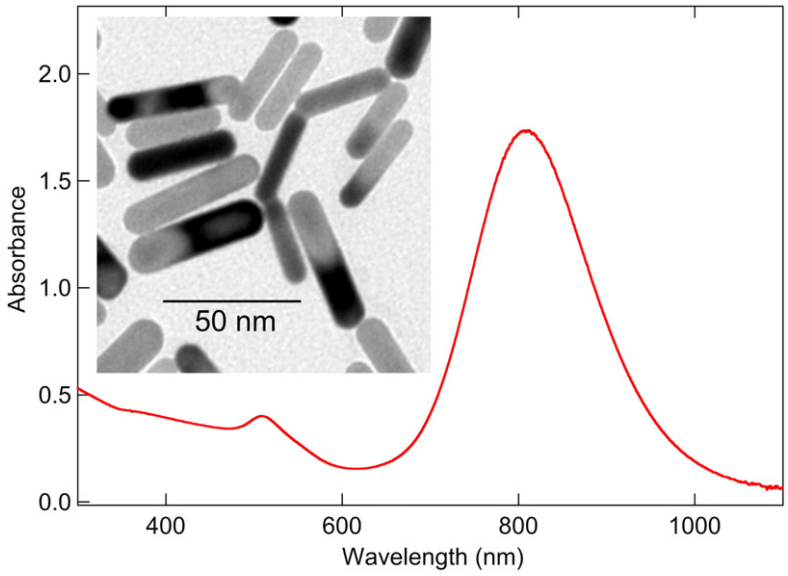

Figure 6. A representative UV–vis spectrum of gold nanorod samples with peak maxima at 509 and 809 nm corresponding to the transverse and longitudinal plasmon modes respectively. The inset shows a representative TEM image.

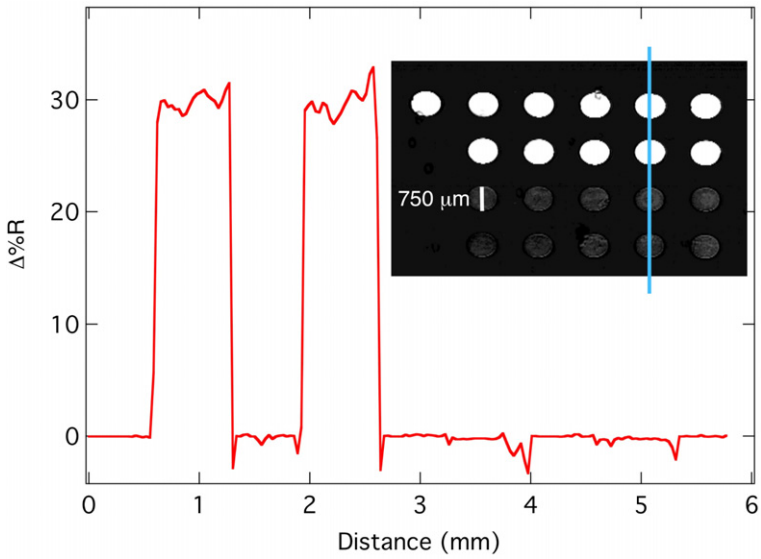

Figure 7. SPRI measurements of the electrostatic adsorption of gold nanorods onto a patterned dsDNA/pLys multilayer. A gold spotted chip was used upon which a first layer of MUAM was self-assembled. For the top two lines of spots, a total of four layers (MUAM, dsDNA, pLys, dsDNA) were created with the bottom two lines consisting of three layers (MUAM, dsDNA, pLys). The inset shows an SPRI difference image obtained for the electrostatic adsorption of gold nanorods. The corresponding line profile plot shows a significant change in $\Delta\%R$ (about 30%) only at spots where dsDNA was the final top layer, with negligible changes in $\Delta\%R$ observed at pLys terminated spots. Each array element has a diameter of 750 μm with a centre-to-centre separation of 1360 μm.

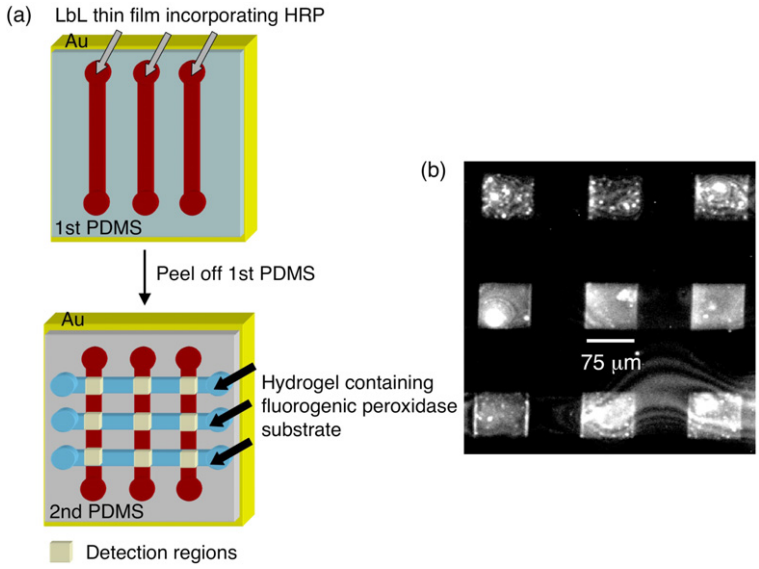

Figure 8. (a) Schematic of a two-step process showing PDMS microfluidic based patterning of the dsDNA/pLys ultrathin films used for the study of an interfacial enzyme reaction. First a set of parallel PDMS microchannels attached to the MUAM modified gold surface was used to create patterned lines of dsDNA/pLys multilayers which were subsequently functionalized with HRP. The first set of microchannels was then replaced with a second set of microchannels orientated perpendicular to the surface line pattern. An agarose solution containing a fluorogenic peroxidase substrate was flowed through each microchannel, which resulted in the creation of a pattern of biopolymer film/hydrogel interfaces. (b) A fluorescence image showing the fluorogenic peroxidase substrate reaction with the HRP incorporated in the dsDNA/pLys film.

Microfluidic patterning and enzyme reactions. As a final example, we have examined an interfacial enzyme reaction between a patterned dsDNA/pLys ultrathin film and a hydrogel layer. Figure 8(a) shows a diagram of the experiment. A parallel set of PDMS microchannels was used to create a three-line pattern of DNA/pLys multilayers on a gold substrate. The dsDNA/pLys multilayers consisted of six monolayers with a terminal pLys monolayer; this film was then reacted with NHS-biotin to create a biotin modified multilayer. Introduction of HRP-avidin to the multilayer attaches HRP onto the three-line pattern. The first set of PDMS microchannels was then removed and a second set of PDMS microchannels was placed perpendicular to the surface line pattern. A hydrogel solution containing a fluorogenic peroxidase substrate was then introduced into the channels, creating a pattern of 75 μm$\times$75 μm thin film/hydrogel interfaces following gelification of the hydrogel solution. Figure 8(b) shows a fluorescence microscope image of the spatially resolved reaction of HRP with QuantaBlu fluorogenic peroxidase substrate. Fluorescence occurs only at the junction between the multilayer film and the hydrogel, demonstrating that an enzymatic reaction occurred across the interface. Since pLys and DNA are easily functionalized, various interesting biomolecules can be potentially incorporated at the biopolymer thin film–hydrogel interface for biosensing.

4. Conclusions

This paper describes the fabrication of well-defined and robust DNA/pLys multilayers on alkanethiol modified gold surfaces which can readily incorporate biomolecules, electroactive

species and nanoparticles. The ultrathin DNA/pLys films can be used in conjunction with various organic electrolyte films and gels to create novel immiscible liquid–liquid interfaces. These interfaces can be easily patterned into multi-element biosensors; we envision the fabrication of novel nucleic acid and protein biosensors based on a combination of bioaffinity binding and ion transport in these interfacial systems. The addition of novel optical materials such as gold nanorods also opens up the possibility of sensors that utilize the electro-optical properties of this unique interface.

Acknowledgments

This research was supported by the National Institute of Health (2RO1 GM059622-04) and the National Science Foundation (CHE-0551935).

References

[1] Decher G 1997 *Science* **277** 1232
[2] Decher G, Lvov Y and Schmitt J 1994 *Thin Solid Films* **244** 772
[3] Lvov Y, Decher G and Mohwald H 1993 *Langmuir* **9** 481
[4] Sukhishvili S A 2005 *Curr. Opin. Colloid Interface Sci.* **10** 37
[5] Hammond P T 2004 *Adv. Mater.* **16** 1271
[6] Bertrand P, Jonas A, Laschewsky A and Legras R 2000 *Macromol. Rapid Commun.* **21** 319–48
[7] Hammond P T 2000 *Curr. Opin. Colloid Interface Sci.* **4** 430–42
[8] Kakkassery J J, Abid J-P, Carrara M and Fermin D J 2004 *Faraday Discuss.* **125** 157–69
[9] Cheng Y, Murtomaki L and Corn R M 2000 *J. Electroanal. Chem.* **483** 88–94
[10] Cheng Y and Corn R M 1999 *J. Phys. Chem.* B **103** 8726
[11] Hoffmannova H, Fermin D, Krtil P and Heyrovsk J 2004 *J. Electroanal. Chem.* **562** 261–5
[12] Slevin C J, Malkia A, Liljeroth P, Toiminen M and Kontturi K 2003 *Langmuir* **19** 1287
[13] Kakkassery J J, Fermin D J and Girault H H 2002 *Chem. Commun.* 1240–1
[14] Ren K, Ji J and Shen J 2006 *Biomaterials* **27** 1152–9
[15] Ren K, Wang Y, Ji J, Lin Q and Shen J 2005 *Colloids Surf.* B **46** 63–9
[16] Ohtake T, Nakamatsu K-I, Shinji Matsui S, Tabata H and Kawai T 2006 *J. Nanosci. Nanotechnol.* **6** 2187–90
[17] van den Beucken J J J P, Vos M R J, Thune P C, Hayakawa T, Fukushima T, Okahata Y, Walboomers X F, Sommerdijk N A J M, Nolte R J M and Jansen J A 2006 *Biomaterials* **27** 691–701
[18] Sukhorukov G B, Mohwald H, Decher G and Lvov Y M 1996 *Thin Solid Films* **284/285** 220
[19] Dootz R, Nie J, Du B, Herminghaus S and Pfohl T 2006 *Langmuir* **22** 1735
[20] Zhang J, Chua L S and Lynn D M 2004 *Langmuir* **20** 8015
[21] Chen X, Lang J and Liu M 2002 *Thin Solid Films* **409** 227–32
[22] Lvov Y M, Lu Z, Schenkman J B, Zu X and Rusling J F 1998 *J. Am. Chem. Soc.* **120** 4073
[23] Lvov Y, Decher G and Sukhorukov G 1993 *Macromolecules* **26** 5396
[24] Brockman J M, Frutos A G and Corn R M 1999 *J. Am. Chem. Soc.* **121** 8044
[25] Lee H J, Nedelkov D and Corn R M 2006 *Anal. Chem.* **78** 6504
[26] Lee H J, Goodrich T T and Corn R M 2001 *Anal. Chem.* **73** 5525
[27] Nikoobakht B and El-Sayed M A 2003 *Chem. Mater.* **15** 1957
[28] Frey B and Corn R M 1996 *Anal. Chem.* **68** 3187
[29] Barner B J, Green M J, Saez E I and Corn R M 1991 *Anal. Chem.* **63** 55
[30] Smith E A and Corn M R 2003 *Appl. Spectrosc.* **57** 320A
[31] Frutos A G, Weibel S C and Corn R M 1999 *Anal. Chem.* **71** 3935
[32] Gerlache M, Senturk Z, Quarin G and Kauffmann J-M 1997 *J. Solid State Electrochem.* **1** 155